

This discussion paper is/has been under review for the journal Atmospheric Measurement Techniques (AMT). Please refer to the corresponding final paper in AMT if available.

# Estimates of Mode-S EHS aircraft derived wind observation errors using triple collocation

S. de Haan

KNMI, Wilhelminalaan 10, De Bilt 3732 GK, the Netherlands

Received: 15 November 2015 – Accepted: 23 November 2015 – Published: 3 December 2015

Correspondence to: S. de Haan (siebren.de.haan@knmi.nl)

Published by Copernicus Publications on behalf of the European Geosciences Union.

AMTD

8, 12633–12661, 2015

Mode-S EHS wind  
observation error

S. de Haan

Title Page

Abstract

Introduction

Conclusions

References

Tables

Figures

◀

▶

◀

▶

Back

Close

Full Screen / Esc

Printer-friendly Version

Interactive Discussion



## Abstract

Information on the accuracy of meteorological observation is essential to assess the applicability of the measurement. In general, accuracy information is difficult to obtain in operational situations, since the truth is unknown. One method to determine this accuracy is by comparison with model equivalent of the observation. The advantage of this method is that all measured parameters can be evaluated, from two meter temperature observation to satellite radiances. The drawback is that these comparisons contain also the (unknown) model error. By applying the so-called triple collocation method (Stoffelen, 1998), on two independent observation at the same location in space and time, combined with model output, and assuming uncorrelated observations, the three error variances can be estimated. This method is applied in this study to estimate wind observation errors from aircraft, obtained using Mode-S EHS (de Haan, 2011). Radial wind measurements from Doppler weather Radar and wind vector measurements from Sodar, together with equivalents from a non-hydrostatic numerical weather prediction model are used to assess the accuracy of the Mode-S EHS wind observations. The Mode-S EHS wind observation error is estimated to be less than  $1.4 \pm 0.1 \text{ m s}^{-1}$  near the surface and around  $1.1 \pm 0.3 \text{ m s}^{-1}$  at 500 hPa.

## 1 Introduction

Quantifying observation errors is of major importance to correctly use or interpret the measured information. For example, the optimal use of observations in assimilation, using variational techniques, is directly related to the assignment of the correct observation error values. A too small error will result in a model initialization which is too tight to the observation, while a too large error will result in a too loose constraint and thus observations will not be optimally exploited. Determining the measurement error can be performed in laboratory environments, which try to mimic the reality as good as possible. Inter comparison studies can also serve as a valuable source for informa-

AMTD

8, 12633–12661, 2015

## Mode-S EHS wind observation error

S. de Haan

[Title Page](#)

[Abstract](#)

[Introduction](#)

[Conclusions](#)

[References](#)

[Tables](#)

[Figures](#)

◀

▶

[Back](#)

[Close](#)

[Full Screen / Esc](#)

[Printer-friendly Version](#)

[Interactive Discussion](#)



tion on the error characteristics of an observation (Nash et al., 2005). Benjamin et al. (1999) compared collocated pairs of aircraft wind observations from Aircraft Communications, Addressing, and Reporting System (ACARS) and showed an observation error of a single horizontal component of wind of  $1.1 \text{ m s}^{-1}$  near the surface and an observation error of  $1.8 \text{ m s}^{-1}$  at 10 km altitude. Drue et al. (2007) showed that systematic deviations in AMDAR wind measurements can be regarded as an error vector, which is fixed to the aircraft reference system. They found systematic deviations in wind measurements from different aircraft types (more than  $0.5 \text{ m s}^{-1}$ ) parallel to the flight direction. Drue et al. (2010) found furthermore a wind vector difference between AMDAR and a radio acoustic sounding system (RASS) of  $2\text{--}2.5 \text{ m s}^{-1}$ . The accuracies found in these studies were relatively to the observed other measurements, and not to a truth which is hard (if not impossible) to measure.

A method to avoid the information on the truth while estimating the uncertainty of three collocated observations in space and time was developed by Stoffelen (1998). The only requirement on the three data sets is that they are not correlated. Most triple collocation data sets consist of two measurement systems and a NWP model. Several studies have been performed using this method (Vogelzang et al., 2011; Roebeling et al., 2012; Draper et al., 2013) for different kind of observation. In this paper the observation error of wind measurements from Mode-S EHS, based on triple collocation with NWP and Sodar or Radar will be presented.

This paper is organized as follows. First the data used is described. Next, the methodology is discussed, that is, the triple collocation method, the method of collocation and the assumptions made are described. This section is followed by the presentation of the results of the triple collocation. The last section is dedicated to the conclusions and outlook.

**Mode-S EHS wind observation error**

S. de Haan

[Title Page](#)[Abstract](#)[Introduction](#)[Conclusions](#)[References](#)[Tables](#)[Figures](#)[|◀](#)[▶|](#)[◀](#)[▶](#)[Back](#)[Close](#)[Full Screen / Esc](#)[Printer-friendly Version](#)[Interactive Discussion](#)

## 2 Data

In this section the data sources used in the present study are described. First a description is given of Mode-S EHS observations, followed by Radar and Sodar. The used NWP model is described finally.

### 5 2.1 Aircraft derived data (Mode-S EHS)

Aircraft are equipped with sensors for flight efficiency and safety. For this purpose, an aircraft measures the speed of the aircraft, its position and ambient temperature and pressure. Since a few decades a selection of these observations are transmitted to a ground station using the AMDAR (Aircraft Meteorological Data Relay) system. An atmospheric profile can be generated when measurements are taken during take-off and landing. See Painting (2003) for more details. Recently, a new type of aircraft-related meteorological information has become available, which originates from observations inferred from a tracking and ranging Radar used for air traffic control. This data is called Mode-S EHS because it is using the Selective enHanced Surveillance Mode of the Radar (<http://mode-s.knmi.nl>; de Haan, 2011).

The difference between Mode-S EHS and AMDAR lies in the method of retrieving the data. AMDAR data is transmitted through a dedicated relay system and AMDAR observations are initiated on request of the meteorological community. Not all aircraft are AMDAR equipped; only selected aircraft have the AMDAR software implemented on their on-board computer. Mode-S EHS observations are received differently, through the aircraft surveillance system triggered by a secondary surveillance Radar (SSR) to track and interrogate aircraft. The SSR sends a request for information on for example aircraft identification, heading, air speed. From this information wind and temperature information can be derived from the position of the aircraft reported by heading, ground track and true air speed. Heading is the direction where the nose of the aircraft points to; true air speed is the speed of the aircraft with respect to air and the ground track is the motion of the aircraft relative to the ground. The wind vector is the difference

[Title Page](#)

[Abstract](#)

[Introduction](#)

[Conclusions](#)

[References](#)

[Tables](#)

[Figures](#)

◀

▶

◀

▶

[Back](#)

[Close](#)

[Full Screen / Esc](#)

[Printer-friendly Version](#)

[Interactive Discussion](#)



between the motion of the aircraft relative to the ground and its motion relative to the air (defined by the airspeed and heading). An SSR has a typical interrogation frequency of once every 4 to 20 s. Consequently, wind and temperature are observed at these same rates. Note that data points are removed by quality control, related to for example turning of the aircraft. Nevertheless a large number of observation pass quality control. See de Haan (2011, 2013) for more details.

## 2.2 Radar and Sodar

A Doppler weather Radar is capable of determining one component of the velocity of scattering particles. Only the velocity component along the line of sight, the so-called radial velocity, can be determined. A Doppler radar is commonly associated with measurements of frequency shifts, because of the low velocities of hydrometeors, however, these shifts cannot be observed directly. The phase of the scattered electromagnetic waves is employed to determine the Doppler frequency shift instead. During pulse-pair processing, the velocity is effectively deduced from the phase jump of the received signal. The unambiguous velocity interval of the instrument, especially for C-band radars, is enhanced by applying a dual pulse repetition frequency (PRF). The two KNMI radars are C-band with a wavelength of 5.3 cm. The high PRF is chosen to be 4/3 of the low PRF, resulting in an unambiguous velocity of four times the low PRF unambiguous velocity, which are  $23 \text{ m s}^{-1}$  for the lowest elevations and  $47 \text{ m s}^{-1}$  for the highest elevations. The PRF also determines the unambiguous range of the Radar, which is 240 km for the lowest elevations and reducing to 120 km for the highest elevations.

A Sodar (Sonic Detection and Ranging) is a ground-based remote sensing instrument for measuring wind and turbulence in the lower atmosphere. A mono-static Sodar is operated and maintained by KNMI at Amsterdam Airport Schiphol (AAS) since March 2006. A Sodar emits short acoustic pulses into the atmosphere and receives atmospheric echoes from turbulent density fluctuations, caused by small-scale temperature or velocity variations. The transmitted signals can be phase shifted to point the beam in different directions. At Schiphol, three are in use for the instrument, one

[Title Page](#)

[Abstract](#)

[Introduction](#)

[Conclusions](#)

[References](#)

[Tables](#)

[Figures](#)

[◀](#)

[▶](#)

[◀](#)

[▶](#)

[Back](#)

[Close](#)

[Full Screen / Esc](#)

[Printer-friendly Version](#)

[Interactive Discussion](#)



10 **2.3 NWP data**

The non-hydrostatic Harmonie (Hirlam ALADIN Research on Mesoscale Operational NWP in Euromed, Seity et al., 2011; Brousseau et al., 2011) model is the follow up of the hydrostatic Hirlam (High resolution limited area model) model; Harmonie explicitly resolves convective processes. The model grid size of the Harmonie model version 15 (cy38h1.2) operational at KNMI is 2.5 km and the Harmonie model is available since early 2012 at KNMI. The model domain covers mainly Western Europe and part of the North Atlantic and the number of grid points is  $800 \times 800$ , meaning that the domain covers a  $2000 \text{ km} \times 2000 \text{ km}$  area. The number of model levels equals 65 with higher density in the lower part of the troposphere. The operational Harmonie model 20 version at KNMI is nested in the European Centre for Medium-Range Weather Forecasts (ECMWF) model. Table 1 lists the Harmonie version used in the study and its main characteristics.

<a href="#">Title Page</a>	
<a href="#">Abstract</a>	<a href="#">Introduction</a>
<a href="#">Conclusions</a>	<a href="#">References</a>
<a href="#">Tables</a>	<a href="#">Figures</a>
<a href="#">◀</a>	<a href="#">▶</a>
<a href="#">◀</a>	<a href="#">▶</a>
<a href="#">Back</a>	<a href="#">Close</a>
<a href="#">Full Screen / Esc</a>	
<a href="#">Printer-friendly Version</a>	
<a href="#">Interactive Discussion</a>	



### 3 Methodology

To perform a triple collocation it is essential that the data sets are collocated in space and time. In this section the method of collocation is described followed by the description of the triple collocation methodology.

5 **3.1 Collocation algorithm**

Observations are collocation in time when the time difference with a three hour forecast of Harmonie is less than 5 min. Note that the model has a three hour cycle, which reduces the collocation time window to 10 min every three hours. We did not interpolate the model to the observation time and the interpolation in space was chosen to be 10 bilinear.

3.1.1 **Radar and Mode-S EHS data collocation method**

The metric of the vertical coordinate, or altitude, of Radar and Mode-S EHS observation differ: Radar radial winds are measured at a certain elevation and range, while altitude of Mode-S EHS is given as flight level. The elevation and range can be converted into position and height altitude (in m), while flight level is easily converted into 15 pressure altitude (in hPa). To enable collocation of a Radar and Mode-S EHS observation, additional information on temperature and humidity profile is needed to convert either pressure into height or vice versa. To perform this conversion, the temperature and humidity profile of an NWP model is used, which is already present at the observation location since NWP is the third data set. This may introduce a correlation between 20 the three data sets, but we think it is negligible.

Given a Mode-S EHS observation location, a matching Radar observation is determined by the following conditions. First of all the distance of the observation location should be at least 50 km away from the Radar, because close to the Radar the radial 25 wind observations have a large error. The Mode-S EHS observation will not perfectly

[Title Page](#)

[Abstract](#)

[Introduction](#)

[Conclusions](#)

[References](#)

[Tables](#)

[Figures](#)

[◀](#)

[▶](#)

[Back](#)

[Close](#)

[Full Screen / Esc](#)

[Printer-friendly Version](#)

[Interactive Discussion](#)



As for Radar, the vertical coordinate of the Soda observation is reported in meters. We used the same algorithm based on the temperature and humidity profile to relate this height to pressure (or actually flight level). The quality indicators, which are output of the Soda processing, are used to screen the Soda observation prior to collocation. Since the Soda is located near the runway, a very close collocation cannot be obtained, we therefore set the maximum distance between the Soda observation and the Mode-S EHS observation to 5 km horizontal and select the Soda observation closest in height.

### 3.2 Triple collocation

We apply the triple collocation method (Stoffelen, 1998) to find quantitative information on the observation error. This method exploits a data set consistent of three co-located measurements of the same parameter. In this paper we use two different wind datasets; the first consist of Mode-S EHS wind vector observation, Sodar and NWP at Schiphol airport and the second dataset consists of Mode-S EHS, Radar radial wind and NWP. The triple collocation method determines simultaneously the linear calibration coefficients and the error of the three datasets under consideration, see Stoffelen (1998).

Title Page	
Abstract	Introduction
Conclusions	References
Tables	Figures
	
	
Back	Close
Full Screen / Esc	
Printer-friendly Version	
Interactive Discussion	



and Vogelzang et al. (2011) for more details. Below, a brief description of the method is given.

5 Assume we have three sets of data  $X_1$ ,  $X_2$  and  $X_3$ , collocated in space and time, where  $X_1$  has the highest resolution and  $X_3$  the lowest resolution. Since the truth is unknown we take data set  $X_1$  as the unbiased reference (or truth). Assume furthermore that two other data sets have a linear relationship with this truth, that is

$$x_1 = t + \epsilon_1, \quad (1)$$

$$x_2 = a_2 t + b_2 + \epsilon_2, \quad (2)$$

$$x_3 = a_3 t + b_3 + \epsilon_3, \quad (3)$$

10 where  $t$  is the truth and  $\epsilon_i$  is the accompanying error, which also contains the representation error, where  $a_i$  and  $b_i$  stand for the trend and bias calibration. Note that each dataset is calibrated against the one with the highest resolution. After calibration, the data sets are transformed into an unbiased dataset, which have an expected value of the error  $\epsilon_i$  equal to zero, that is

15  $\langle \epsilon_i \rangle = 0, \quad (4)$

where  $\langle \rangle$  denotes the expected value. Assume furthermore that the variance of the errors,  $\langle \epsilon_i^2 \rangle$ , is independent of the truth  $t$  and has a Gaussian signature. As stated by Stoffelen (1998) this is true for the zonal and meridional wind components but not for wind speed and direction. In this paper we use additionally the radial wind component, which is a projection of wind vector on a (varying) azimuth angle, and thus the variance is expected to be independent of the true wind vector with a Gaussian error distribution.

20 The representativeness of the three observation most likely differ; there is a residual correlation error  $r^2$  of the scales that are represented by the high resolution observations but are lacking in the relatively low resolution NWP wind retrievals. Using all above stated assumptions we are able to find estimates for the unknowns  $a_i$  and  $b_i$ , that is, with  $M_i$ ,  $M_{ij}$  and  $c_{ij}$  the first and second (mixed) moment, and co-variance,

[Title Page](#)

[Abstract](#)

[Introduction](#)

[Conclusions](#)

[References](#)

[Tables](#)

[Figures](#)

[◀](#)

[▶](#)

[Back](#)

[Close](#)

[Full Screen / Esc](#)

[Printer-friendly Version](#)

[Interactive Discussion](#)



defined as

$$M_i = \langle x_i \rangle, M_{ij} = \langle x_i x_j \rangle \text{ and } c_{ij} = M_{ij} - M_i M_j, \quad (5)$$

the unknowns become

$$a_2 = c_{23}/c_{31} \text{ and } a_3 = c_{23}/(c_{12} - a_2 r^2) \quad (6)$$

5  $b_2 = M_2 - a_2 M_1$  and  $b_3 = M_3 - a_3 M_1.$  (7)

Using these values we find that

$$\sigma_1^2 = c_{11} - c_{31} c_{12}/c_{23} + r^2 \quad (8)$$

$$\sigma_2^2 = c_{22}/a_2^2 - c_{31} c_{12}/c_{23} + r^2 \quad (9)$$

$$\sigma_z^2 = c_{33}/a_3^2 - c_{31} c_{12}/c_{23}. \quad (10)$$

10 The only unknown now still is the residual correlation error  $r^2$ . This correlation can be determined by a scale analysis of Mode-S EHS and NWP, following Vogelzang et al. (2011).

The data sets we use in this study consist of wind vector data (Mode-S EHS/Sodar/NWP) and radial wind (Mode-S EHS/Radar/NWP). For both data sets we 15 need to determine the residual correlation error  $r^2$ . Figure 2a shows the power spectral density (PSD) for the zonal component of the wind from Mode-S EHS (solid line, top) and Harmonie (dashed bottom line). This graph is constructed using nine months of Mode-S EHS collocations with Harmonie. The PSD is calculated using Mode-S EHS data from aircraft which reported wind for more than 100 km in length at a stable height.

20 The thin dashed line shows the  $-5/3$  Kolmogorov spectral decay. The PSD from Mode-S EHS lies close to this line, while the Harmonie PSD is clearly lower displaying the lack of energy in the model at these scales. The area between these PSD represents the variance lacking in the model that is present in the observations; this area is approximately  $r^2 = 0.312 \text{ m}^2 \text{ s}^{-2}$ . Figure 2b shows a similar plot but now for the simulated

[Title Page](#)

[Abstract](#)

[Introduction](#)

[Conclusions](#)

[References](#)

[Tables](#)

[Figures](#)

◀

▶

[Back](#)

[Close](#)

[Full Screen / Esc](#)

[Printer-friendly Version](#)

[Interactive Discussion](#)



radial wind. We have used the distribution of azimuth angles in the Radar radial wind data set to create a radial wind data set from NWP and Mode-S EHS. The area between the PSD for radial wind is around  $r^2 = 0.285 \text{ m}^2 \text{ s}^{-2}$ .

Stoffelen (1998) estimated the representation error for buoys and scatterometer winds with respect to the ECMWF model to be  $r^2 = 0.75 \text{ m}^2 \text{ s}^{-2}$ . This value is much higher than is found for Harmonie in this study. The difference can not fully be explained by the difference observation (10 m vs. upper air wind), nor in model resolution, nor in the fact that Harmonie is a convection resolving model. Moreover, since Harmonie uses ECMWF boundaries, upper air characteristics from Harmonie are linked to the ECMWF model. The difference in representation error needs further research, but is not discussed here.

The representative error has some relation to the azimuth angle (zonal component of the wind is equal to a radial wind observed with an azimuth angle of 90°), see Fig. 3. Each point in this figure is based on the mean value of PSD determined from the data set of wind vectors mapped to the radial component using a prescribed azimuth. Not surprisingly the residual error exhibits a bi-periodic behaviour which is due to the fact that the errors of opposite vectors are identical. Also shown in this figure is the residual correlation when converting the wind vector to a radial wind component using the distribution of azimuth angles observed in the Mode-S EHS/Radar data set. The resulting residual correlation error lies close to the mean value of the azimuthal residual errors.

## 4 Results

### 4.1 Mode-S EHS and Sodar wind observation error

Now that we have estimated the residual error we can use the triple collocation method to determine the observation errors. Figure 4 shows the observation error of Mode-S EHS and Sodar for different azimuth angles. From the original wind vector a ra-

[Title Page](#)

[Abstract](#)

[Introduction](#)

[Conclusions](#)

[References](#)

[Tables](#)

[Figures](#)

[◀](#)

[▶](#)

[Back](#)

[Close](#)

[Full Screen / Esc](#)

[Printer-friendly Version](#)

[Interactive Discussion](#)



## Mode-S EHS wind observation error

S. de Haan

Title Page

Abstract

Introduction

Conclusions

References

Tables

Figures

|◀

▶|

◀

▶

Back

Close

Full Screen / Esc

Printer-friendly Version

Interactive Discussion



## 4.2 Mode-S EHS, Radar and Sodar wind observation error

The radial wind is equal to the zonal component of the wind for an azimuth angle of 90 and 270°. Similarly, the radial wind for an azimuth of 0 or 180° equals the meridional component. By selecting in the Mode-S EHS/Radar/NWP data set azimuth angles between 75 and 105° (and 255 to 285°) we can make an estimate of the zonal component of the wind error of Mode-S EHS at levels higher than the Sodar. The result is shown in Table 2. These statistics show consistency between both triple collocation data sets when taking into account the observed uncertainty of the estimates. Due to the small numbers of Mode-S EHS observations satisfying the azimuth angle conditions the uncertainty for the estimates based on the Mode-S EHS/Radar/NWP dataset is larger than for the other triple collocation dataset (for the latter all observations can be used obviously). The uncertainty range of the Mode-S EHS/Radar/NWP estimates overlaps the uncertainty of the Mode-S EHS/Sodar/NWP. The Mode-S EHS error is approximately 1.4 to 1.5 m s<sup>-1</sup> near the surface. Note that the zonal Mode-S EHS observations are found at a higher altitude, which, as we will see later, influences the magnitude of the error slightly. The meridional component statistics, shown also in Table 2, are obtained by selecting angles smaller than 15° and larger than 345° azimuth, and between 165 and 195° azimuth. The estimate of the observation error is larger than the one for the zonal component but the difference is of the order 0.1 m s<sup>-1</sup>. Again the uncertainty of the Mode-S EHS/Radar/NWP observation error is larger than the uncertainty from the other data set, and again there is a clear overlap of the uncertainty intervals.

The result of the triple collocation for all radial wind component is shown in Fig. 6. The error bar denotes again the spread of the triple collocation standard deviation estimates by dividing the data sets into 10 subsets and estimate the observation error for each subset.

The lowest data point originates from the triple collocation of Mode-S EHS/Sodar/NWP, where we created radial wind observation from the wind vectors using the azimuth distribution as observed by the other data set. The other data points

## Mode-S EHS wind observation error

S. de Haan

[Title Page](#)

[Abstract](#)

[Introduction](#)

[Conclusions](#)

[References](#)

[Tables](#)

[Figures](#)

◀

▶

◀

▶

[Back](#)

[Close](#)

[Full Screen / Esc](#)

[Printer-friendly Version](#)

[Interactive Discussion](#)



in Fig. 6 are based on triple collocation of radial wind observations from the Mode-S EHS/Radar/NWP dataset. Apart from levels higher than 600 hPa the estimated error is slightly below  $1.5 \text{ m s}^{-1}$ . The higher levels deviate from  $1.5 \text{ m s}^{-1}$  which is related to the distribution of the azimuth angles used to estimate the Mode-S EHS observation error, as can be seen in Fig. 7, where the azimuth distribution is shown in bins of  $30^\circ$  for the different height bins. It is clear from this figure that the two highest estimates (higher than 600 hPa in Fig. 6, the triangles in Fig. 7) have a clear different signature in azimuth distribution than the lower four estimates. Because the azimuth distributions differ substantially, the reconstructed radial wind dataset of the highest levels is not consistent with that of the lowest levels. The distribution of the azimuth angles will influence the magnitude of the observation error estimate (see Fig. 4). In order to have a better comparison between error estimates at different levels, a re sampling of the datasets is performed, such that the azimuth distribution for each level matches the azimuth distribution of the whole data set. We used the distribution in  $30^\circ$  bins as a reference. Figure 8 shows the re-sampled distributions. When two or more observed azimuth values are present in the original bin, the re-sampled bin is filled by randomly sampling (with replacement) from this bin until the number found is exactly equal to that of the reference bin. Note that when a bin contains none or only one azimuth value this bin is skipped. When this occurs, it will influence the number data points in the other bins, because the total number of data points of all bins is kept constant. The consequence is that the azimuthal distributions will differ from the reference distribution, as can be seen in Fig. 8 for the azimuth distribution of the lowest level (960 hPa, open square) and the highest level (538 hPa, solid triangle). All other new azimuth distributions match the reference very good (Fig. 8). The resulting estimates of Mode-S EHS observation error after re-sampling is shown in Fig. 9. Again, each dataset is sub-divided into 10 subsets which are subsequently used to estimate the uncertainty of the observation error estimate using triple collocation. In general the estimates are slightly smaller than without re-sampling, while the estimate uncertainty is slightly larger, especially for the highest level. The overall increase in uncertainty is related to over-sampling of the dataset.

S. de Haan

[Title Page](#)

[Abstract](#)

[Introduction](#)

[Conclusions](#)

[References](#)

[Tables](#)

[Figures](#)

[◀](#)

[▶](#)

[◀](#)

[▶](#)

[Back](#)

[Close](#)

[Full Screen / Esc](#)

[Printer-friendly Version](#)

[Interactive Discussion](#)



For example, the increase of uncertainty observed for the top level is due to the relatively small number of data points in the height bin for this level. It appears that the observation error is decreasing with height above 800 hPa. The numbers used in the triple collocation increase also slightly because of the re-sampling, which selects multiple data points from an under-sampled (original) bin.

Finally, we present the trend and bias for the re-sampled radial wind data sets, see Table 3. Again the trend of Mode-S EHS is around 1 with a small uncertainty obtained by splitting the data set into 10 subsets. The bias is between  $-0.1$  and  $0.4 \text{ ms}^{-1}$  with an uncertainty of around  $0.2 \text{ ms}^{-1}$ . The trend in NWP is smaller than 1, apart from the highest level. The bias is in general positive between 0 and  $0.4 \text{ ms}^{-1}$  with an uncertainty of around  $0.2 \text{ ms}^{-1}$  (again except the highest level). These numbers are in agreement with the previous trend and bias estimates presented in Fig. 5.

## 5 Conclusions and outlook

In this study we applied the triple collocation technique to estimate the Mode-S EHS observation error. We used two triple datasets consisting of Mode-S EHS/Sodar and NWP, and Mode-S EHS, Radar and NWP. Using the first dataset an estimate of the two horizontal wind vector components was found for observations with an altitude of at most 700 m. The estimated observation error for the wind components was around  $1.40 \text{ ms}^{-1}$  for the zonal component of the wind and  $1.45 \text{ ms}^{-1}$  for the meridional component of the wind. The uncertainty of these estimates is  $0.1 \text{ ms}^{-1}$ . The second data set is used to estimate the Mode-S EHS observation along the line of sight of a Radar beam. Using this data set knowledge was gained on the vertical behaviour of the observation error. It turns out the the radial wind observation error is not constant with azimuth angle, but that the Mode-S EHS observation error of the zonal and meridional component are more or less equal to each other and to the Mode-S EHS observation error constructed using the actual azimuth angle distribution.

[Title Page](#)

[Abstract](#)

[Introduction](#)

[Conclusions](#)

[References](#)

[Tables](#)

[Figures](#)

[◀](#)

[▶](#)

[◀](#)

[▶](#)

[Back](#)

[Close](#)

[Full Screen / Esc](#)

[Printer-friendly Version](#)

[Interactive Discussion](#)



The observation error of Mode-S EHS wind vector projected on the radial component has some dependence on height. The projection is performed using the distribution of the azimuth as observed in the Mode-S EHS/Radar/NWP data set. It appears that, after re-sampling, from the surface to 800 hPa the observation error is between 1.2 to 5  $1.4 \text{ m s}^{-1}$ , while from 800 to 500 hPa the error decreases from approximately 1.5 to  $1.1 \text{ m s}^{-1}$ , however the uncertainty of the observation error estimate increases with increasing height.

10 Simultaneously with the estimation of the wind vector error for Mode-S EHS, the error of Sodar is estimated. It turns out that the wind vector from Sodar is of good quality and therefore could be used for assimilation in Harmonie. The triple collocation method can also be used to determine observation error correlation when the measurement systems have a good spatial coverage at collocated time.

**Acknowledgements.** EUROCONTROL Maastricht Upper Area Control Centre (MUAC) is kindly acknowledged for the provision of the ASTERIX CAT048 data.

## 15 References

Benjamin, S. G., Schwartz, B. E., and Cole, R. E.: Accuracy of ACARS wind and temperature observations determined by collocation, *Weather Forecast.*, 14, 1032–1038, doi:10.1175/1520-0434(1999)014<1032:AOAWAT>2.0.CO;2, 1999. 12635

20 Brousseau, P., Berre, L., Bouttier, F., and Desroziers, G.: Background-error covariances for a convective-scale data-assimilation system: AROME–France 3D-Var, *Q. J. Roy. Meteor. Soc.*, 137, 409–422, doi:10.1002/qj.750, 2011. 12638

de Haan, S.: High-resolution wind and temperature observations from aircraft tracked by Mode-S air traffic control radar, *J. Geophys. Res.*, 116, D10111, doi:10.1029/2010JD015264, 2011. 12634, 12636, 12637

25 de Haan, S.: An improved correction method for high quality wind and temperature ob servations derived from Mode-S EHS, Tech. Rep. TR338, Koninklijk Nederlands Meteorologisch Instituut, De Bilt, the Netherlands, 2013. 12637

Title Page

Abstract

Introduction

Conclusions

References

Tables

Figures

|◀

▶|

◀

▶

Back

Close

Full Screen / Esc

Printer-friendly Version

Interactive Discussion



Draper, C., Reichle, R., de Jeu, R., Naeimi, V., Parinussa, R., and Wagner, W.: Estimating root mean square errors in remotely sensed soil moisture over continental scale domains, *Remote Sens. Environ.*, 137, 288–298, 2013. 12635

Drüe, C., Frey, W., Hoff, A., and Hauf, T.: Aircraft type-specific errors in AMDAR weather reports from commercial aircraft, *Q. J. Roy. Meteor. Soc.*, 134, 229–239, 2007. 12635

5 Drüe, C., Hauf, T., and Hoff, A.: Comparison of boundary-layer profiles and layer detection by AMDAR and WTR/RASS at Frankfurt airport, *Bound.-Lay. Meteorol.*, 135, 407–432, 2010. 12635

10 Nash, J., Smout, R., Oakley, T., Pathack, B., and Kurnosenko, S.: WMO intercomparison of high quality radiosonde systems, Vacoas, Mauritius, 2–25 February 2005, WMO Report no. 1303, World Meteorological Organization, Geneva, Switzerland, 115 pp., 2005. 12635

Painting, J. D.: WMO AMDAR Reference Manual, WMO Report-no.958, World Meteorological Organization, Geneva, Switzerland, available at: <http://www.wmo.int> (last access: 1 December 2015), 2003. 12636

15 Roebeling, R., Wolters, E., Meirink, J., and Leijnse, H.: Triple collocation of summer precipitation retrievals from SEVIRI over Europe with gridded rain gauge and weather radar data, *J. Hydrometeorol.*, 13, 1552–1566, 2012. 12635

Seity, Y., Brousseau, P., Malardel, S., Hello, G., Bénard, P., Bouttier, F., Lac, C., and Masson, V.: The AROME-France convective-scale operational model, *Mon. Weather Rev.*, 139, 976–991, 20 doi:10.1175/2010MWR3425.1, 2011. 12638

20 Stoffelen, A.: Toward the true near-surface wind speed: error modeling and calibration using triple collocation, *J. Geophys. Res.-Oceans*, 103, 7755–7766, 1998. 12634, 12635, 12640, 12641, 12643

25 Vogelzang, J., Stoffelen, A., Verhoef, A., and Figa-Saldaña, J.: On the quality of high-resolution scatterometer winds, *J. Geophys. Res.-Oceans*, 116, C10033, doi:10.1029/2010JC006640, 2011. 12635, 12641, 12642

## Mode-S EHS wind observation error

S. de Haan

Title Page

Abstract

Introduction

Conclusions

References

Tables

Figures

|◀

▶|

◀

▶

Back

Close

Full Screen / Esc

Printer-friendly Version

Interactive Discussion



**Table 1.** Harmonie main characteristics.

Model Version	38h1.2
Horizontal resolution	2.5 km
Cycle	3 h
Observation window	3 h
Lateral Boundaries	ECMWF
Assimilation	3DVAR
Observations	SYNOP (pressure) AMDAR (temperature, wind) Radiosonde (temperature, humidity, wind)

<a href="#">Title Page</a>	
<a href="#">Abstract</a>	<a href="#">Introduction</a>
<a href="#">Conclusions</a>	<a href="#">References</a>
<a href="#">Tables</a>	<a href="#">Figures</a>
<a href="#">◀</a>	<a href="#">▶</a>
<a href="#">◀</a>	<a href="#">▶</a>
<a href="#">Back</a>	<a href="#">Close</a>
<a href="#">Full Screen / Esc</a>	
<a href="#">Printer-friendly Version</a>	
<a href="#">Interactive Discussion</a>	



**Table 2.** Mode-S EHS wind component observation error estimate.

zonal component			
	level	number	estimated error
Mode-S EHS (Radar/NWP)	913–422 hPa	118	$1.23 \pm 0.41$
Mode-S EHS (Sodar/NWP)	0–700 m	2403	$1.40 \pm 0.10$
meridional component			
	level	number	estimated error
Mode-S EHS (Radar/NWP)	962–480 hPa	599	$1.38 \pm 0.20$
Mode-S EHS (Sodar/NWP)	0–700 m	2403	$1.45 \pm 0.10$

[Title Page](#) [Abstract](#) [Introduction](#)  
[Conclusions](#) [References](#)  
[Tables](#) [Figures](#)

[◀](#) [▶](#)  
[◀](#) [▶](#)  
[Back](#) [Close](#)

[Full Screen / Esc](#)

[Printer-friendly Version](#)  
[Interactive Discussion](#)



**Table 3.** Trend and bias for re-sampled radial wind.

	height	number	$a_{\text{EHS}}$ [-]	$b_{\text{EHS}}$ [ $\text{ms}^{-1}$ ]	$a_{\text{NWP}}$ [-]	$b_{\text{NWP}}$ [ $\text{ms}^{-1}$ ]
Radar	541 hPa	487	$1.01 \pm 0.03$	$-0.06 \pm 0.19$	$1.02 \pm 0.05$	$0.30 \pm 0.67$
	611 hPa	965	$1.00 \pm 0.03$	$0.37 \pm 0.25$	$0.97 \pm 0.05$	$0.25 \pm 0.29$
	685 hPa	1299	$0.97 \pm 0.01$	$-0.12 \pm 0.21$	$0.96 \pm 0.02$	$0.09 \pm 0.23$
	769 hPa	1886	$0.97 \pm 0.02$	$0.04 \pm 0.28$	$0.96 \pm 0.02$	$0.16 \pm 0.23$
	867 hPa	2716	$1.05 \pm 0.03$	$-0.02 \pm 0.13$	$0.98 \pm 0.03$	$-0.05 \pm 0.10$
	927 hPa	1043	$0.99 \pm 0.05$	$0.28 \pm 0.24$	$0.97 \pm 0.05$	$0.39 \pm 0.20$
Sodar	987 hPa	2406	$1.00 \pm 0.02$	$0.20 \pm 0.18$	$0.97 \pm 0.02$	$-0.09 \pm 0.10$

Title Page

Abstract

Introduction

Conclusions

References

Tables

Figures

◀

▶

◀

▶

Back Close

Full Screen / Esc

Printer-friendly Version

Interactive Discussion



## Discussion Paper | Mode-S EHS wind observation error

S. de Haan

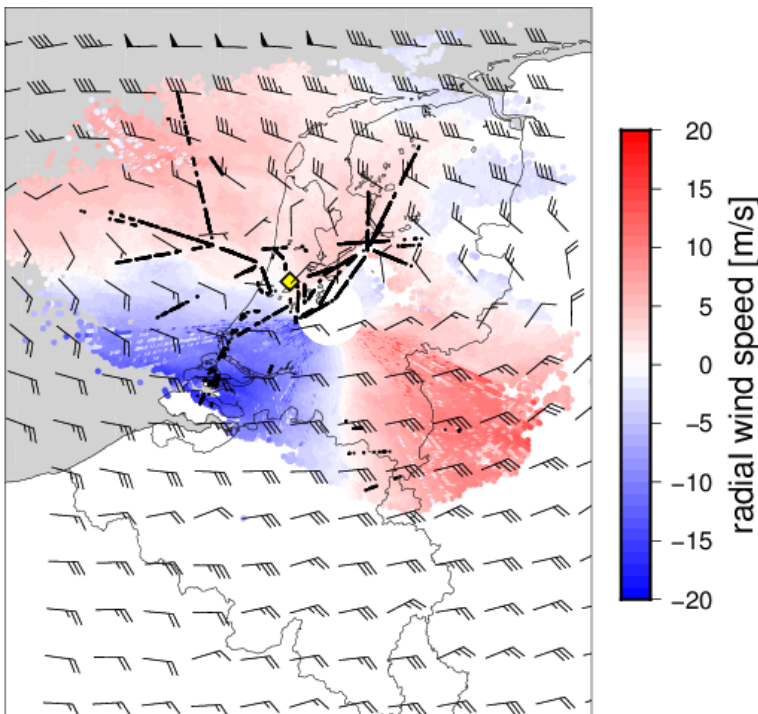


**Figure 1.** Radial wind speed from the Doppler weather Radar in De Bilt, location of the Sodar (marked by the yellow diamond), Mode-S EHS observations (black dots), and Harmonie (thinned) wind field at approximately 850 hPa; all valid on 9 March 2013 12:00 UTC.

## Mode-S EHS wind observation error

S. de Haan

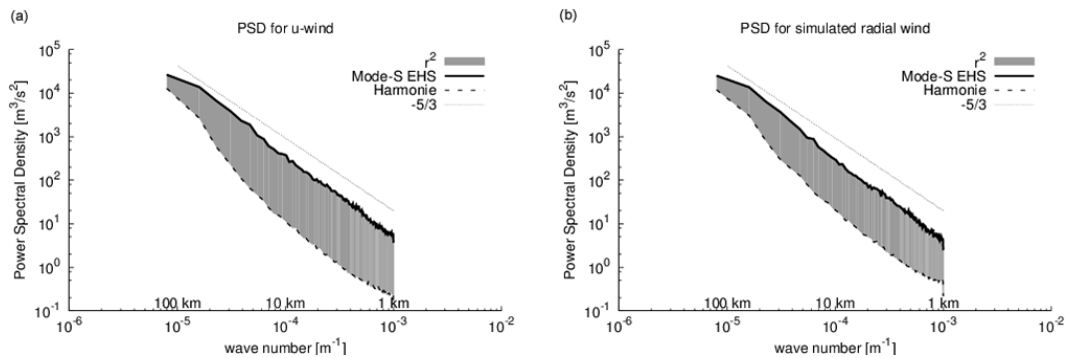


**Figure 2.** Power spectral density of **(a)** zonal component and **(b)** radial wind component of Mode-S EHS and Harmonie. The shaded area represents the difference radial wind variance of Mode-S EHS and Harmonie for scales roughly between 1 and 100 km.

[Title Page](#)[Abstract](#)[Introduction](#)[Conclusions](#)[References](#)[Tables](#)[Figures](#)[|◀](#)[▶|](#)[Back](#)[Close](#)[Full Screen / Esc](#)[Printer-friendly Version](#)[Interactive Discussion](#)

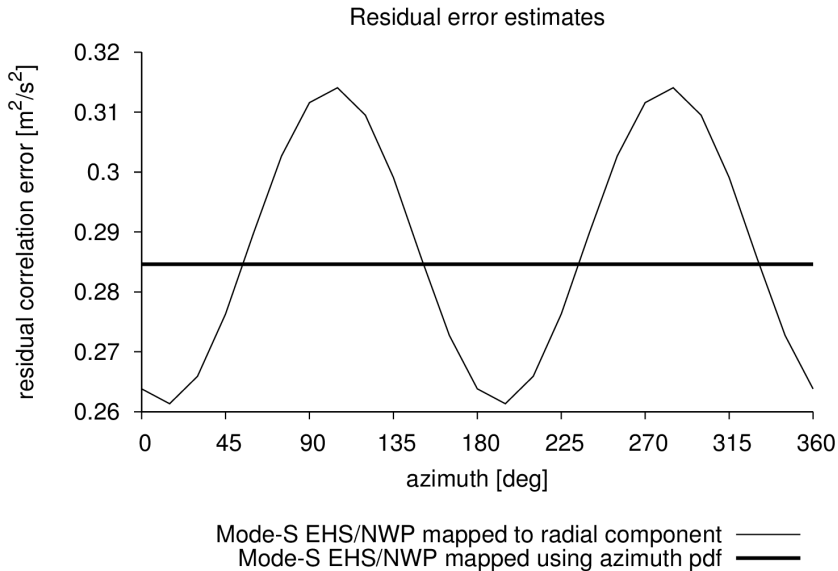


**Figure 3.** The residual error as a function to the azimuth angle. A data set consisting of nine month of Mode-S EHS collocations with Harmonie was used to create a data set of radial wind for each azimuth angle. The solid straight line shows the residual error using the observed distribution of azimuth angles in the Mode-S EHS/Radar/NWP data set.

## Mode-S EHS wind observation error

S. de Haan

[Title Page](#)

[Abstract](#)

[Introduction](#)

[Conclusions](#)

[References](#)

[Tables](#)

[Figures](#)

◀

▶

[Back](#)

[Close](#)

[Full Screen / Esc](#)

[Printer-friendly Version](#)

[Interactive Discussion](#)



## Mode-S EHS wind observation error

S. de Haan

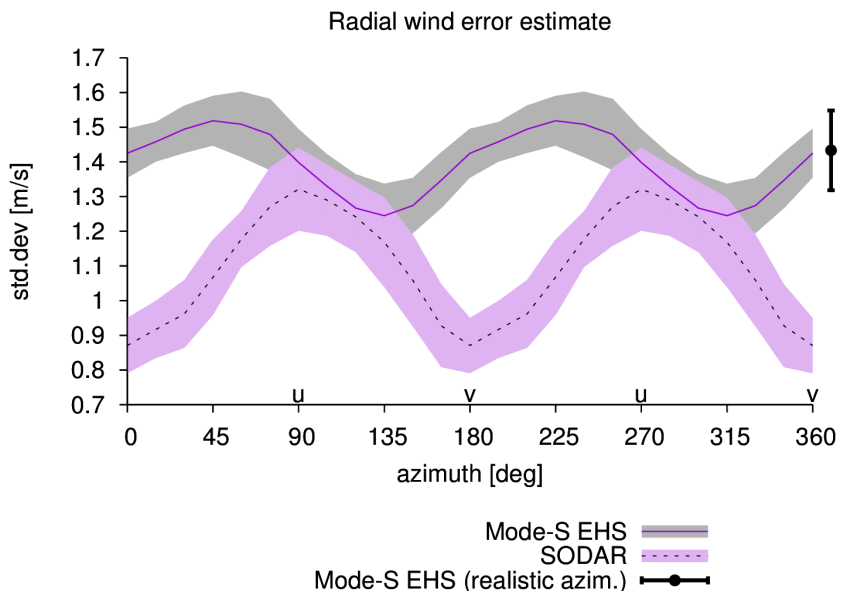


**Figure 4.** Error estimates of radial wind component for Mode-S EHS and Sodar based wind vector observations for different azimuth angles. The black vertical error bar indicates the radial wind error estimate from Mode-S EHS with the radial wind component constructed from the wind vector using the azimuth distribution of the Radar data set.

[Title Page](#)[Abstract](#)[Introduction](#)[Conclusions](#)[References](#)[Tables](#)[Figures](#)[|◀](#)[▶|](#)[◀](#)[▶](#)[Back](#)[Close](#)[Full Screen / Esc](#)[Printer-friendly Version](#)[Interactive Discussion](#)

## Mode-S EHS wind observation error

S. de Haan

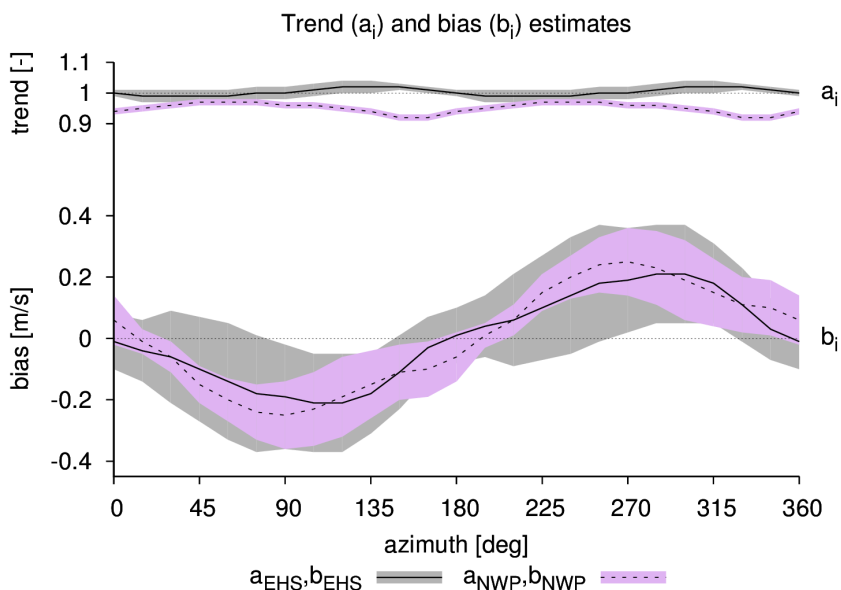


**Figure 5.** Trend and bias of the Mode-S EHS and NWP radial wind component triple collocation for different azimuth angles.

[Title Page](#)[Abstract](#)[Introduction](#)[Conclusions](#)[References](#)[Tables](#)[Figures](#)[◀](#)[▶](#)[◀](#)[▶](#)[Back](#)[Close](#)[Full Screen / Esc](#)[Printer-friendly Version](#)[Interactive Discussion](#)

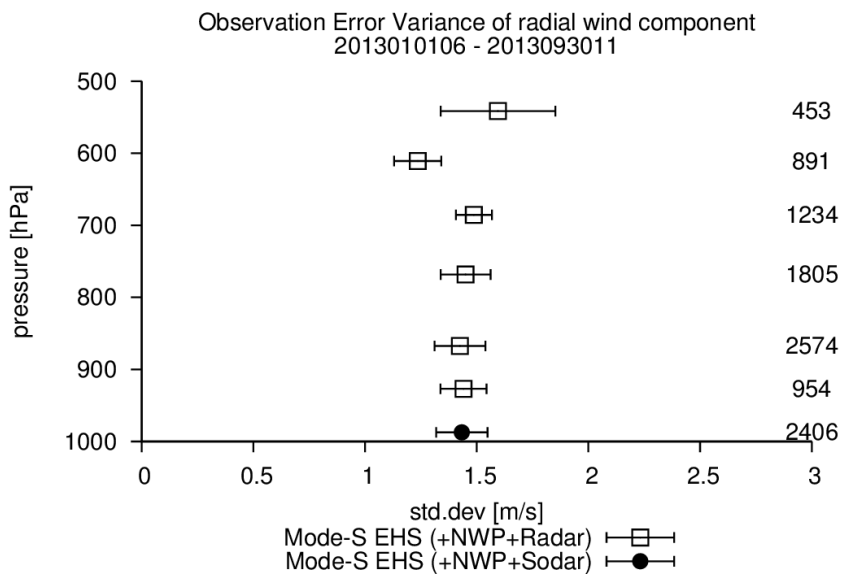


**Figure 6.** Mode-S EHS radial wind error estimates from the two triple collocation data sets with respect to height. Error bar indicates the uncertainty of the error estimates based on error estimates determined from 10 subsets.

## Mode-S EHS wind observation error

S. de Haan

[Title Page](#)

[Abstract](#)

[Introduction](#)

[Conclusions](#)

[References](#)

[Tables](#)

[Figures](#)

◀

▶

◀

▶

[Back](#)

[Close](#)

[Full Screen / Esc](#)

[Printer-friendly Version](#)

[Interactive Discussion](#)



## Mode-S EHS wind observation error

S. de Haan

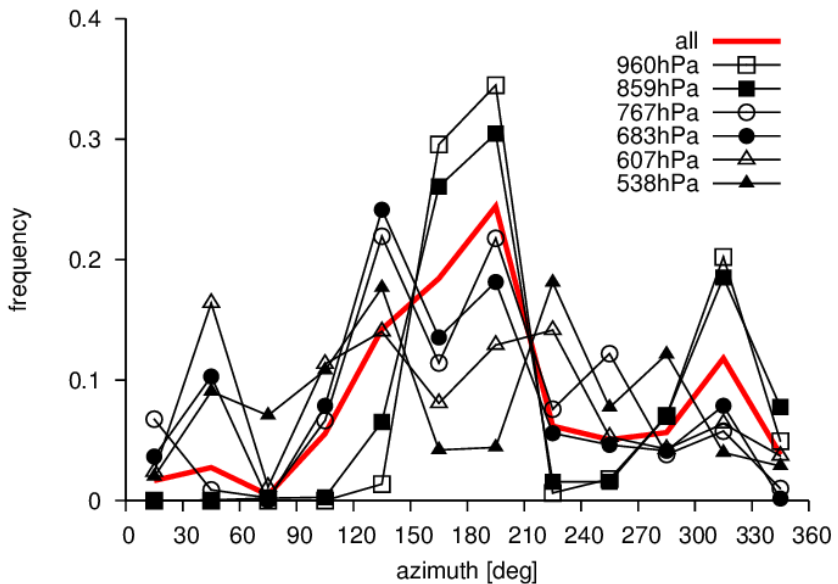


**Figure 7.** Azimuthal distribution of the datasets used to estimate the Mode-S EHS observation error for different heights; in red is the azimuth distribution of the complete data set. Azimuth bin is set to 30°.

## Mode-S EHS wind observation error

S. de Haan

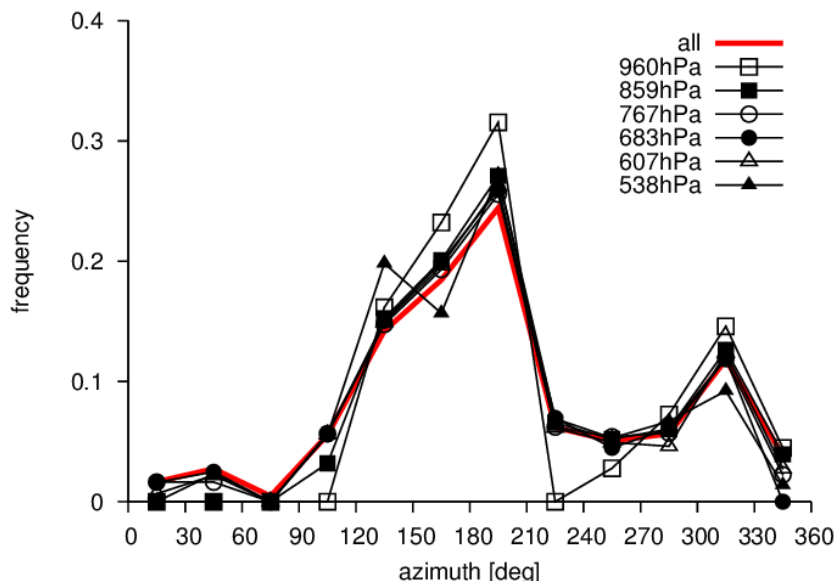


**Figure 8.** Azimuthal distribution of the re-sampled datasets. Azimuth bin is set to 30°.

<a href="#">Title Page</a>	<a href="#">Discussion Paper</a>
<a href="#">Abstract</a>	<a href="#">Introduction</a>
<a href="#">Conclusions</a>	<a href="#">References</a>
<a href="#">Tables</a>	<a href="#">Figures</a>
<a href="#">◀</a>	<a href="#">▶</a>
<a href="#">◀</a>	<a href="#">▶</a>
<a href="#">Back</a>	<a href="#">Close</a>
<a href="#">Full Screen / Esc</a>	
<a href="#">Printer-friendly Version</a>	
<a href="#">Interactive Discussion</a>	



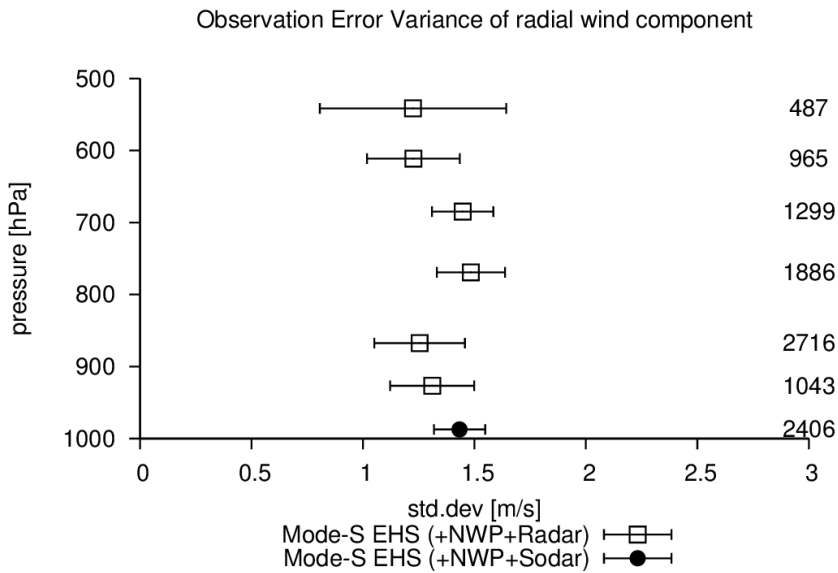


**Figure 9.** Mode-S EHS radial wind error estimates from the two triple collocation data sets with respect to height. The Mode-S EHS/Radar/NWP data set has been re-sampled to have similar azimuth distributions. Error bar indicates the uncertainty of the error estimates based on error estimates determined from 10 subsets.

## Mode-S EHS wind observation error

S. de Haan

[Title Page](#)

[Abstract](#)

[Introduction](#)

[Conclusions](#)

[References](#)

[Tables](#)

[Figures](#)

◀

▶

◀

▶

[Back](#)

[Close](#)

[Full Screen / Esc](#)

[Printer-friendly Version](#)

[Interactive Discussion](#)

